Structure-based models for determining the mechanical properties of plant cell walls

Hung Kha[1,2]**, Sigrid Tuble**[1,2]**, Shankar Kalyanasundaram**[2] **and Richard E. Williamson**[1]

[1]*Research School of Biological Sciences, Australian National University, Canberra*
[2]*Department of Engineering, Australian National University, Canberra*

Abstract: The mechanical properties of the primary cell wall strongly influence plant growth and the final shapes of plant cells. Little attention has been paid to the relationship between the composite structure of the wall and its stiffness properties. In this study, a finite element model has been developed to predict the effective Young's modulus of elasticity for a "simplified" primary wall composed of microfibrils cross-linked by hemicelluloses (typically xyloglucans). The assembled cellulose-xyloglucan network forms the input for finite element analysis once the two polymer types and the bonds between them are assigned realistic mechanical properties. The size of the model was varied to obtain a Representative Volume Element so that homogenization techniques could be developed for further investigations. The Young's modulus of elasticity decreases as the dimensions of the simulated wall increase but then settles to a steady value.

Keywords: cell wall, finite element analysis (FEA), cellulose microfibril (CMF), xyloglucan (XG).

1 Introduction

Wood and cotton are two familiar materials that owe their value to plant cell walls. Only cells that have stopped growing can lay down the thick secondary walls that form these materials. Before this can happen, cells deposit weaker primary walls (often only ~100µm thick) whose mechanical properties determine how fast and in what directions the cell – and so the plant – can grow [1]. Plants grow into their varied shapes by continuous fine tuning of the mechanical properties of their primary walls. We want to understand how wall microstructure and composition determines wall mechanics and hence plant growth.

Current views of wall structure and mechanics postulate two mechanically significant networks, the first comprising cellulose microfibrils interlinked with hemicellulose chains and the second comprising a network of pectic polysaccharides [2]. These views reflect the integration of structural studies (e.g. X-ray diffraction, electron and atomic force microscopy), studies of how polysaccharides bind to each other *in vitro*, analysis of the conditions required to release individual polysaccharides from cell walls and analysis of how removing specific polysaccharides (by selective extraction or genetic mutation) affects wall structure and mechanics. Cellulose microfibrils (CMFs) dominate wall microstructure [1,2]. Each CMF is a semi-crystalline aggregate of about 36 β-1,4-glucan chains. CMFs are several µm long but only about 3nm thick and lie 20-30µm apart in the wall. Cells can control CMF orientation and, as with other fibre composites, a preferred alignment creates mechanical anisotropy that minimises deformation in the direction parallel to the high stiffness values. Hemicelluloses such as xyloglucans (XGs) interlink the CMFs [1,2]. This chemically heterogeneous class of polysaccharides has medium length chains (~100nm) of which an average of 25nm at each end might be linked by hydrogen bonds to a CMF. To grow, cells must expand their encasing cell wall and they apply the required forces by actively accumulating solutes so causing osmotic water uptake. That puts cell contents under substantial positive pressures (~0.5MPa) and leads to walls carrying tensile stresses of ~50MPa. Walls grow by controlled deformation to those stresses. Further deposition of CMFs and XGs reinforce the stretching wall allowing wall area to increase by ≥ 30 fold without rupture. Deformation of CMFs and XG chains themselves will be minor relative to the overall length changes accompanying growth. The latter is thought to necessitate breaking H-bonds to peel XGs off CMFs and/or using enzymes to cleave covalent bonds and so cut XG chains. The two processes are collectively termed "wall loosening" and the cell regulates its rate of expansion by controlling them [1]. Pectins, a chemically heterogeneous class of branched polysaccharides, form a second network ramifying through the spaces within the CMF-XG network [2, 3]. They are mechanically significant but may be less important in regulating the rate of expansion than the peeling and cutting of XGs and less important than CMF orientation in regulating the anisotropy of expansion.

Plants create and remodel walls to control the rate of expansion (area doubling times range from tens of minutes to many days) and its anisotropy (small isodiametric cells can expand into the long, narrow cells making a grass leaf, into isodiametric cells making a potato and into every shape in between). There are many qualitative hypotheses for how wall structure and composition affect wall mechanical properties and hence growth but there is no quantitative understanding of their relationship. We want to predict quantitatively how changing composition and microstructure will alter mechanical properties so generating this diversity of growth rates and shapes. We use a multi-scale modelling approach in which we construct a virtual cell wall (currently comprising CMFs and XGs only) in which we specify composition and structure on the nm scale, assign mechanical properties to its components and using finite element analysis (FEA), predict the mechanical properties of wall fragments whose sizes are measured on the μm scale that is relevant to plant growth. We can vary the composition and microstructure of the virtual wall allowing us to rapidly explore how changes alter wall mechanics.

In this initial study, we describe a FE approach to determine stiffness properties of the primary wall typical of a species such as *Arabidopsis thaliana*, a plant commonly used for cell wall research [2]. The influence of the size of the wall fragment used on the effective Young's modulus of elasticity was examined.

2 Methods

The FE method [4] was employed to predict the deformed shape of a primary wall under applied loading. Geometry and boundary conditions of the wall were generated (using a program written in Fortran) and imported into HyperMesh (a pre- and post-processing software for FE codes) [5] to assign mechanical properties to the CMFs and the XGs. OptiStruct (a FE code) [5] was used to solve for the equations of linear static analysis for the wall. Results from OptiStruct were used to calculate the effective Young's modulus of elasticity of the wall using another Fortran-based program.

2.1 Reconstruction of primary wall geometry and prescribing boundary conditions

PCWNetGen (a program written in Fortran) was used to reconstruct the geometry of a fragment of primary wall. Primary walls show considerable variation in detailed structure but our starting point has been the thin walls characteristic of many plant organs. These are about 100 μm thick and comprise some 3 or 4 layers of microfibrils [2]. The program consists of a number of subroutines which generate beam elements representing CMFs and XGs and their connectivity. The operator controls parameters such as the number of layers comprising the wall, the size of the CMFs and XGs, their volume fraction and overall orientation. The program first places CMFs sequentially at randomly selected sites and rejects any CMF whose ends lie too close to the end of an existing CMF. (This allows CMFs to cross as seen in electron micrographs of primary walls). CMF generation continues until the specified volume fraction for CMFs is achieved. XGs are then added by a similar process and connected to CMFs where they intersect. XGs failing to intersect two CMFs or lying too close to an existing XG are rejected. Portions of XGs extending beyond the junctions with CMFs are trimmed off. Figure 1 shows a FE model of one layer of a primary wall which might have four layers in total. It contains CMFs (red beams) and XGs (blue beams). An enlarged view of CMF-XG connectivity is shown in Fig. 2. In this study, the volume fraction of the CMFs was 0.012; each CMF was 2000nm in length (both figures likely to be towards the lower end of the range occurring *in vivo*) and 3.2nm in both thickness and width. CMFs were assumed not to interact with each other but were cross-linked by XGs each of which was 65nm in length and 0.5nm in both thickness and width. The minimum separation distance between the ends of any two CMFs was 30nm, while that between the ends of any two XGs was 15nm. In the example shown in Figs. 1 and 2, CMFs and XGs were randomly oriented by setting a large standard deviation for their orientation. Because of the requirement that XGs are only retained if they contact two CMFs, XGs are absent from regions where CMFs are well spaced and cluster where CMFs are more closely spaced.
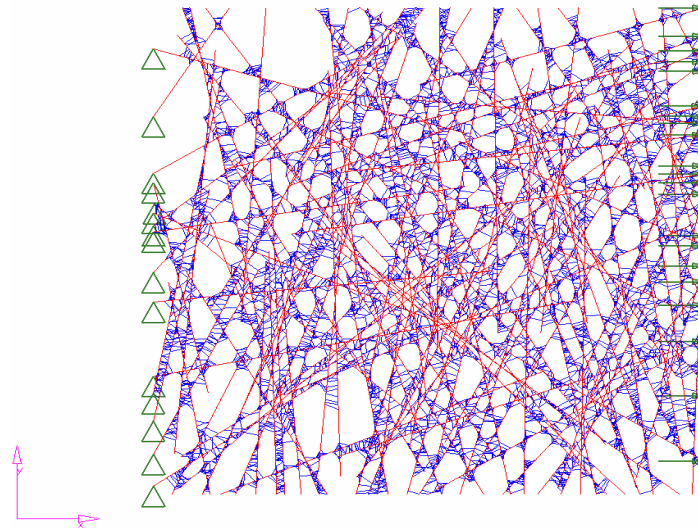
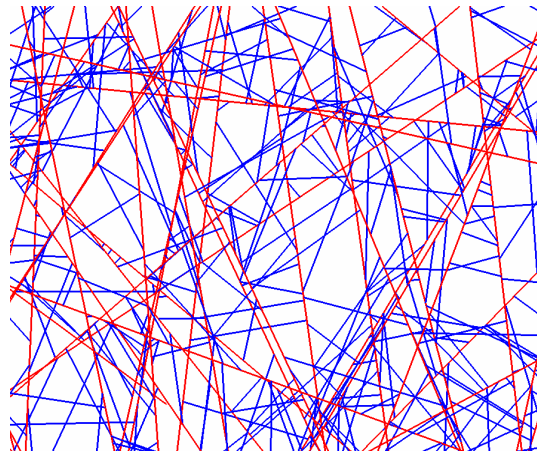Fig. 1. A FE model of a 'simplified' primary wall of *Arabidopsis thaliana*.

Fig. 2. Enlarged view of a small part of the primary wall shown in Fig. 1.

The program PCWNetGen can generate complex walls consisting of a series of layers interconnected by XGs and resembling the lamellae seen *in vivo* where the layers would be separated by a 20-30nm space filled by pectins and other polysaccharides. For simplicity, only a single layered wall was used in the current examples. In estimating its thickness for calculating the effective elastic modulus, we assumed that the narrow layer of CMFs and XGs was surrounded by pectin-filled space as would be the case *in vivo*.

The program PCWNetGen was also used to prescribe boundary conditions for each wall model. Nodes of the beam elements lying at the left edge of the wall were fixed and displacements along the x-direction were applied to the nodes of the elements at the opposite edge, as shown by the green triangles and arrows in Fig. 1.

2.2 Assigning mechanical properties and implementing FEA

HyperWorks (a FEA software package) [5] was used to assign the mechanical properties of individual polysaccharides (CMFs and XGs) and to implement FEA to study the deformation of the wall fragment. Young's moduli of elasticity of 30 and 0.1 GPa [6] were assigned to the CMFs and XGs, respectively, in HyperMesh (a pre- and post-processor of HyperWorks). A Poisson ratio of 0.3 was adopted for both CMFs and XGs. A linear static analysis was implemented by solving Equations (1a) and (1b) using OptiStruct (a FE code within HyperWorks) [5].

$$Ku = P \qquad (1a)$$

where K = stiffness matrix; u = displacement vector; P = vector of load.

$$\sigma = C\varepsilon \qquad (1b)$$

where σ = stress; C = elasticity matrix; ε = strain (function of displacement).

2.3 Calculation of effective Young's modulus

Effective Young's modulus of elasticity of the wall was calculated using the following equation:

$$E = \frac{F}{A} \times \frac{L}{\Delta L} \qquad (2)$$

where

        ΔL = change in length of the wall fragment along x-axis after the wall deformed (nm)
        L = original length of the wall fragment along the x-axis (nm)
        A = cross-sectional area of one side of the wall fragment (nm^2)
        F = average force (N) = sum of all single point constraint forces of nodes (obtained from the analysis described in Section 2.2)

HMAnalysis (another Fortran program) was written and used to calculate the effective Young's modulus E. The original length L and the cross-sectional area A were obtained for this program by importing the input file of the PCWNetGen program (used for generating geometry and prescribing boundary conditions, as shown in Section 2.1), while the input and the output files of OptiStruct (FEA – Section 2.2) were imported into the program to provide the average force F and the change in length ΔL.

3 Results and discussion

Figure 3 shows the deformed shape of the primary wall fragment. As expected, the wall extended in the x-direction and contracted in the y-direction due to the applied tension at the right edge of the wall (Fig. 1). The colours represent different levels of deformation of the polysaccharides from lowest (dark blue) to highest (red), as shown in the legend at the top left corner (unit in nm). The applied loads caused relatively large displacements (yellow areas) at the right edge of the wall fragment and smaller deformations at the constrained left edge (blue areas).
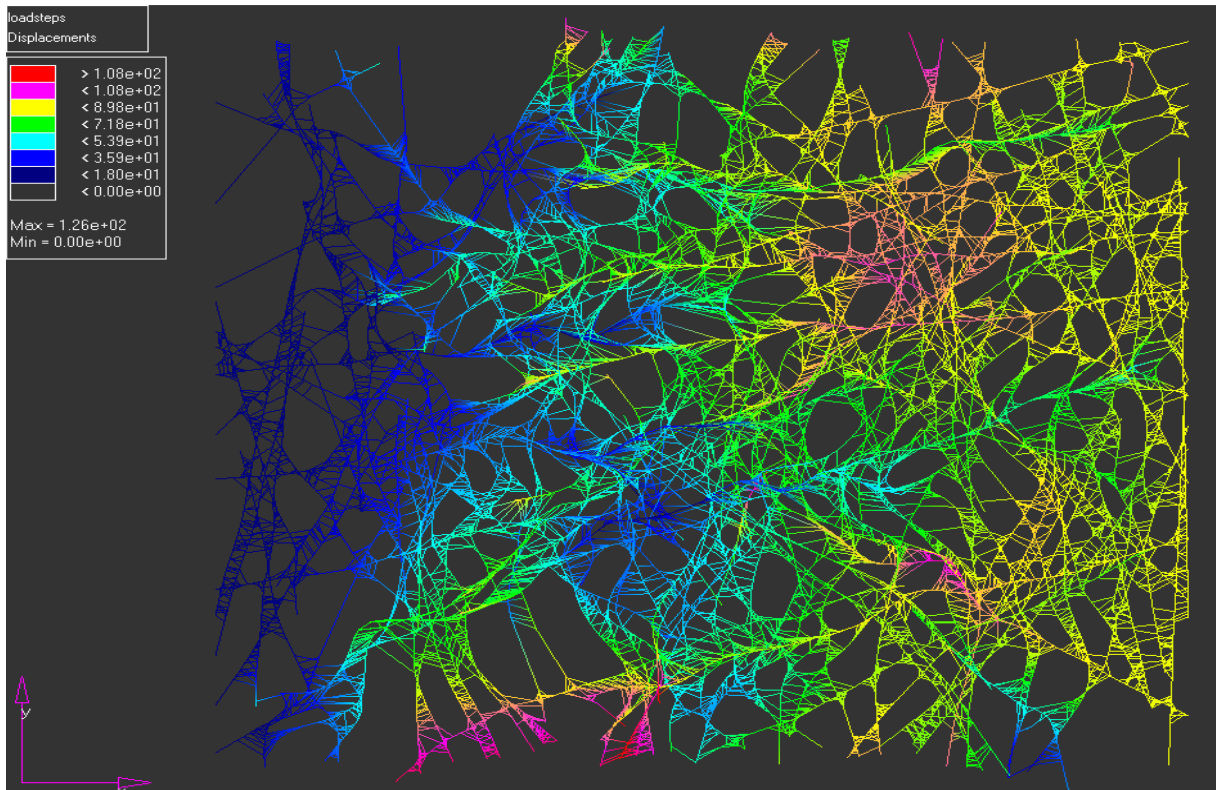

Fig. 3. Deformed shape of the primary wall.

We first investigated how the effective Young's modulus varied with the size of the virtual wall fragment that was analysed. The program PCWNetGen was used to generate square wall fragments with sides ranging from 1,200nm to 9,600nm. The number of beam elements (CMFs and XGs) ranged from 10,240 to 639,559 in the different sized fragments. Since the program places CMFs at random sites in space, no two walls have exactly the same microstructure even when they have the same volume fraction, CMF orientation etc. Therefore, the generation of wall geometry was repeated five times for models of each size to study the variability in effective Young's modulus.

Results from the FE model showed that the Young's modulus was relatively high (~29MPa) for a fragment with a side of 1,200nm and decreased to a steady value of ~3MPa in the larger wall fragments (Fig. 4). The high value for the small fragments probably results from the CMFs, which were 2000nm long, extending the full width of the wall fragment and so dominating its mechanical properties. As the size of the wall fragment increases, the effective modulus falls reflecting the influence of XGs, the second type beam element to which we assigned a lower Young's modulus. The effective modulus estimated for the large wall fragments is towards the lower end of the range reported from experimental measurements of walls from which pectins have been extracted to leave only the CMFs and XGs that we are modelling [7].
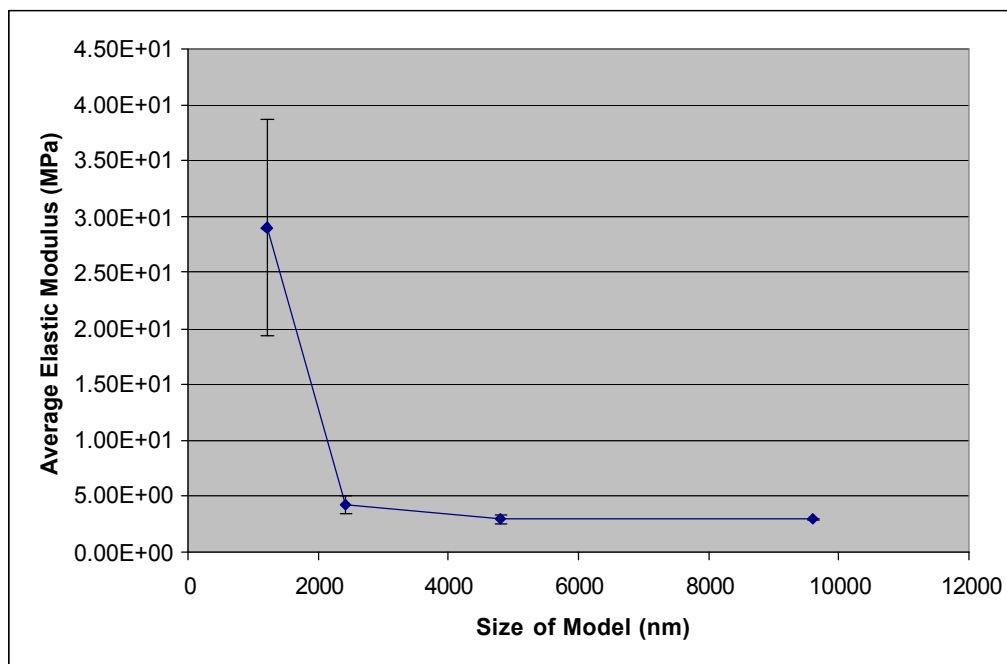

Fig. 4. Young's modulus of elasticity of a 'simplified' *Arabidopsis thaliana* primary wall at different wall sizes. Points are mean ± standard error for n=5.

The size of the error bars in Fig. 4 show that the variability in the estimates of effective modulus rapidly decreased as the size of the wall fragments increased presumably reflecting the much smaller influence of stochastic differences in the microstructure of replicate walls.

4 Conclusions and recommendations for further work

In this study, a FE model has been developed to predict stiffness properties of networks consisting of the two of the main polysaccharide components of the primary wall that might occur in a species such as *Arabidopsis thaliana*. The model has been used to predict deformation of the wall under applied loads, thereby allowing the calculation of its effective Young's modulus of elasticity. The modulus settles to a steady value once the size of the fragment used reaches about 5,000nm. The predicted value is at the lower end of the range measured experimentally.

A major limitation of the current program is that it links CMFs and XGs rigidly rather than through the relatively weak hydrogen bonds that exist *in vivo* and which will break under mechanical loads. The next refinement of PCWNetGen will simulate weak bonds between the two types of beam element which will break under mechanical loading. These weak bonds will in turn allow us to use higher

elastic moduli for XG in line with measurements made on fully extended chains by atomic force microscopy. Beyond that, we hope further refinements will embody wall loosening reactions and incorporate pectins that also contribute to the mechanical properties of real cell walls. The models will allow us to rapidly explore how changes in wall composition and microstructure affect predicted mechanical properties and how plants control their growth. Our efforts are initially focused on primary walls and our future work will focus on very complicated structure, for example, helicoidally arranged microfibrils [8]. In addition, suitable modifications to allow for different microstructure and composition would allow PCWNetGen to build and analy ze secondary walls.

Acknowledgement

References

[1] Cosgrove D. J. 2005. Growth of the plant cell wall. Nat Rev Mol Cell Biol 6, 850-861.

[2] Sommerville C., Bauer S., Brininstool G., Facette M., Hamann T., Milne J., Osbourne E., Paredez A., Persson S., Raab T., Vorwerk S., Youngs H., 2004. Toward a systems approach to understanding plant cell walls. Science 306, 2206-2211.

[3] Ridley B.L., O'Neill M.A., Mohnen D., 2001. Pectins: structure, biosynthesis and oligogalacturonide-related signalling. Phytochemistry 57, 929-967.

[4] Zienkiewicz, O. C., 1977. The Finite Element Method. 3rd ed. McGraw-Hill, United Kingdom.

[5] Altair Engineering, 2007. HyperWorks Version 8.0 User's Manual. USA.

[6] Eichhorn SJ, Young RJ. 2001. The Young's modulus of a microcrystalline cellulose. Cellulose 8, 197-207.

[7] Ryden P., Sugimoto-Shirazu K., Smith A.C., Findlay K., Reiter W.-D., McCann M.C., 2003. Tensile properties of Arabidopsis cell walls depend on both a xyloglucan cross-linked microfibrillar network and rhamnogalacturonan II-borate complexes. Plant Physiology 132, 1033-1040.

[8] Roland J.C., Reis D., Vian B., Roy S. 1989. The helicoidal plant-cell wall as a performing cellulose-based composite. Biology of the Cell 67, 209-220.